EUROPEAN ORGANIZATION FOR NUCLEAR RESEARCH
CERN — AB DEPARTMENT

CERN-AB-Note-2006-016 ATB

Development of an Ionization Scheme for Gold using the Selective Laser Ion Source at the On-Line Isotope Separator ISOLDE

V.N. Fedosseev

CERN, CH-1211, Geneva-23, Switzerland

P. Kosuri

KTH, Stockholm SE-100 44, Sweden

B.A. Marsh

CERN, CH-1211, Geneva-23, Switzerland,
The University of Manchester, Manchester M13 9PL, United Kingdom

Abstract

At the ISOLDE on-line isotope separation facility, the resonance ionization laser ion source (RILIS) can be used to ionize reaction products as they effuse from the target. The RILIS process of laser step-wise resonance ionization of atoms in a hot metal cavity provides a highly element selective stage in the preparation of the radioactive ion beam. As a result, the ISOLDE mass separators can provide beams of a chosen isotope with greatly reduced isobaric contamination. The number of elements available at RILIS has been extended to 26, with the addition of a new three-step ionization scheme for gold. The optimal ionization scheme was determined during an extensive study of the atomic energy levels and auto-ionizing states of gold, carried out by means of in-source resonance ionization spectroscopy. Details of the ionization scheme and a summary of the spectroscopy study are presented.

Geneva, Switzerland
17th March 2006

1 Introduction

ISOLDE is an isotope separator on-line (ISOL) type radioactive ion beam facility. Radioactive atoms are produced in a thick target during its bombardment by a high-energy proton beam. Isotope separation of the ionized reaction products takes place as the ion beam passes through a magnetic mass separator. This process alone does not provide a chemically pure beam since many isobars may be present at the chosen mass. Thus, an additional separation between nuclides with different proton number Z is favoured for many applications of the radioactive ion beams. This can be performed by chemical methods, using the different chemical behavior of different elements. Alternatively, an atomic physics technique, step-wise resonance photo-ionization, can be used. At the ISOLDE facility, the Resonance Ionization Laser Ion Source (RILIS) exploits the unique electronic structure of different atomic species to provide a rapid, efficient and Z – selective ionization process [1, 2]. In principle, the RILIS can be used for the ionization of almost all metallic elements and an important aspect of ongoing development is the extension of its range with the study of resonance ionization schemes. Recently a request for the development of gold ion beams was addressed to the ISOLDE and Neutron Time of Flight Experiments Committee (INTC) by the letter of intent "Study of the $\pi h^{-1}_{11/2}$ isomeric states in ^{201,203,205}Au". Following an endorsement of this intent by the committee, the task of finding an efficient RILIS ionization scheme for gold was put forward.

Resonance ionization spectroscopy has been applied for gold by several groups. The data obtained as well as the ionization schemes used are compiled by E.B. Saloman [3]. In particular, an efficient ionization scheme with a three-colour, three-step excitation to an autoionizing state has been used for on-line laser spectroscopy of laser-desorbed gold isotopes [4, 5]. Autoionizing states of Au were also studied by resonance ionization spectroscopy in [6, 7]. Since the RILIS laser system and the conditions in the ionization region are different from those used in [4, 6, 7], investigating the performance of these known schemes at the RILIS setup was necessary. In addition, the search for transitions to the autoionizing states was carried out in these works for only a few excited states in a limited spectral range, which is not readily available at RILIS. Therefore, a new, more extensive study of gold resonance ionization at the RILIS setup was required for defining the optimal ionization scheme.

In this article we present results of the resonance ionization spectroscopy study of gold atomic transitions performed at the RILIS setup. Based on the experimental results, the optimal ionization scheme is defined. A summary is presented along with details of this new ionization scheme.

2 The Resonance Ionization Laser Ion Source

References [2, 8, 9] give a thorough description of the ISOLDE RILIS. A master oscillator – power amplifier system of copper vapor lasers (CVL) operating at the pulse repetition rate of 11 kHz provides two output laser beams, each with an average power of typically 30-40 W. The RILIS set-up includes three dye lasers and therefore ionization schemes employing up to 3 resonant transitions can be used. The wavelength range of the dye lasers is 530-850 nm. Frequency doubling and tripling of dye laser beams are carried out using non-linear BBO (beta-barium borate) crystals to generate 2nd or 3rd harmonics of the fundamental beam, extending the wavelength range to include 214-415 nm. This enables high lying first excited states to be attained and is essential for elements with a high ionization potential. With this current work included, the RILIS has been used for resonance ionization of 26 of the elements. Schemes using one, two or three resonant transitions have been used.

Most commonly, the ionization step is a transition to the continuum using an available CVL beam. Alternatively, the final step can be a resonant transition to an auto-ionizing state. A transition to an auto-ionizing state can have a high cross section, which is favorable for improving the ionization efficiency.

Ionization takes place in a hot cavity connected to the target. Reaction products enter this cavity as an atomic vapor at a temperature of around 2300 K. The role of the cavity is to contain the atoms for a certain time within a volume where they can be irradiated by the laser light and to confine the ions during their drift towards the extraction region. The ionization cavities are refractory metal (W or Nb) tubes with an inner diameter of 3 mm and a length of typically 30 mm. They are resistively heated to a temperature of about 2300K with a DC current of 200–350 A. After leaving the source, ions are accelerated to 60 kV, separated in a magnetic field and guided by electrostatic ion-optical elements to the experimental setup.

For this work, a standard ISOLDE target was used with a tungsten surface ionizer cavity. The target/ion source unit was equipped with two ovens. A large Au sample was placed in one of these, for use during the initial spectroscopy study and ionization scheme search. The second oven was loaded with a precise 3000 nAh Au sample, for use during the final efficiency measurement. The mass separator was tuned to the mass of ^{197}Au and the transmitted ion current was monitored on a Faraday cup detector.

3 Resonance Ionization Spectroscopy of Gold

Data on atomic lines and energy levels for Au are taken from the Kurucz atomic line database [10]. The ionization potential for gold (9.23 eV) is high with respect to the photon energy-range attainable with RILIS (~ 1.7 – 5 eV). As a result, ionization schemes using three excitation steps were investigated. For the first step, the transitions from the ground state $\boldsymbol{6s\ ^2S_{1/2}}$ to the levels $\boldsymbol{6p\ ^2P_{1/2}}$ and $\boldsymbol{6p\ ^2P_{3/2}}$ at 37358.991 cm^{-1} and 41174.613 cm^{-1} respectively are the only known transitions that can be reached with the RILIS laser system. Both transitions are strong and of similar strength (A = $1.65\cdot10^8$ s^{-1} and $1.96\cdot10^8$ s^{-1}). At 242.868 nm, the wavelength required to populate the 41174.613 cm^{-1} level is at the short wavelength end of the RILIS tuning range and can be generated only by tripling the fundamental frequency of the dye laser. The efficiency of 3rd harmonic generation is low (< 5% for a 5W fundamental beam) and so, if this transition is used, a large proportion of the CVL pump beam power must be used to obtain the dye laser power required at the fundamental frequency. The transition to the lower lying, $\boldsymbol{^2P_{1/2}}$ level is preferable since the transition energy, 37358.991 cm^{-1}, corresponds to that of a 267.673 nm photon, accessible by 2nd harmonic generation of light at 535.198 nm. This falls within the emission range of the Pyrromethene 546 dye, which is pumped with the green component of the CVL beam. Measurements were carried out using only this transition for the first step in the excitation scheme.

From this first excited state, 11 potential second excited states from 54485 cm^{-1} to 72164 cm^{-1} are documented [10]. All but the lowest lying of these excited states exist at an energy of less than 19581 cm^{-1} below the continuum, meaning that ionization from these levels is possible via non-resonant absorption of a 511 nm photon, provided by the green CVL beam. Accessing any of these 10 transitions requires 2nd harmonic generation of the fundamental dye laser beam, and hence, a significant proportion of CVL pump power. It is preferable to use all of the CVL pump power at 511 nm for the generation of the frequency for the first transition and for the final ionization stage, leaving only the yellow (578 nm) component for the second step. Therefore, we have limited our study to the group of six second step transitions (Figure 1), which are accessible with a frequency doubled dye laser pumped with light at 578 nm.

The pumping requirements of the dye lasers and amplifiers for the first and second step transitions were met using the total output of the higher power of the two CVL amplifiers after separation of the yellow and green components of the beam. Typical values of the average power for this CVL beam were 22 W and 20 W at 511 nm and 578 nm respectively. The second CVL beam with a total power (in both components) of 27 W was available for the last excitation step.

As the first stage of this study, schemes using 3-step ionization with a non-resonant transition to the continuum (induced by both the green and the yellow components of the CVL beam) were studied. During this study, an ion current of gold was observed in the presence of only the beam for the first step in the excitation scheme. Since the ionization threshold of Au (74409.0(2) cm^{-1} [11]) is slightly less than the sum of the energies of two photons at 267.673 nm, this ion current is attributed to the occurrence of two-step ionization via a transition to the continuum from the first excited state by non-resonant absorption of second photon from the first step beam. The presence of this laser-ionized ion signal facilitated a reliable optimization of the beam focusing and positioning. In addition, the measurements of the ion current produced by the first step transition beam provided a useful reference point for use in the evaluation of the relative efficiencies of ionization schemes. The ratio of ion current produced with three laser beams versus ion current produced by the first step beam $\boldsymbol{R = I_{1+2+3}/I_{1+3}}$ is taken as an efficiency parameter of the

ionization scheme. In order to keep thermal conditions of laser beam transport optics constant these measurements were carried out whilst blocking only the beam of second step laser, leaving the most powerful laser beam propagating toward the ion source. This beam did not participate in the ionization process because its photon energy was less than required for transition from the first excited state to the ionization continuum.

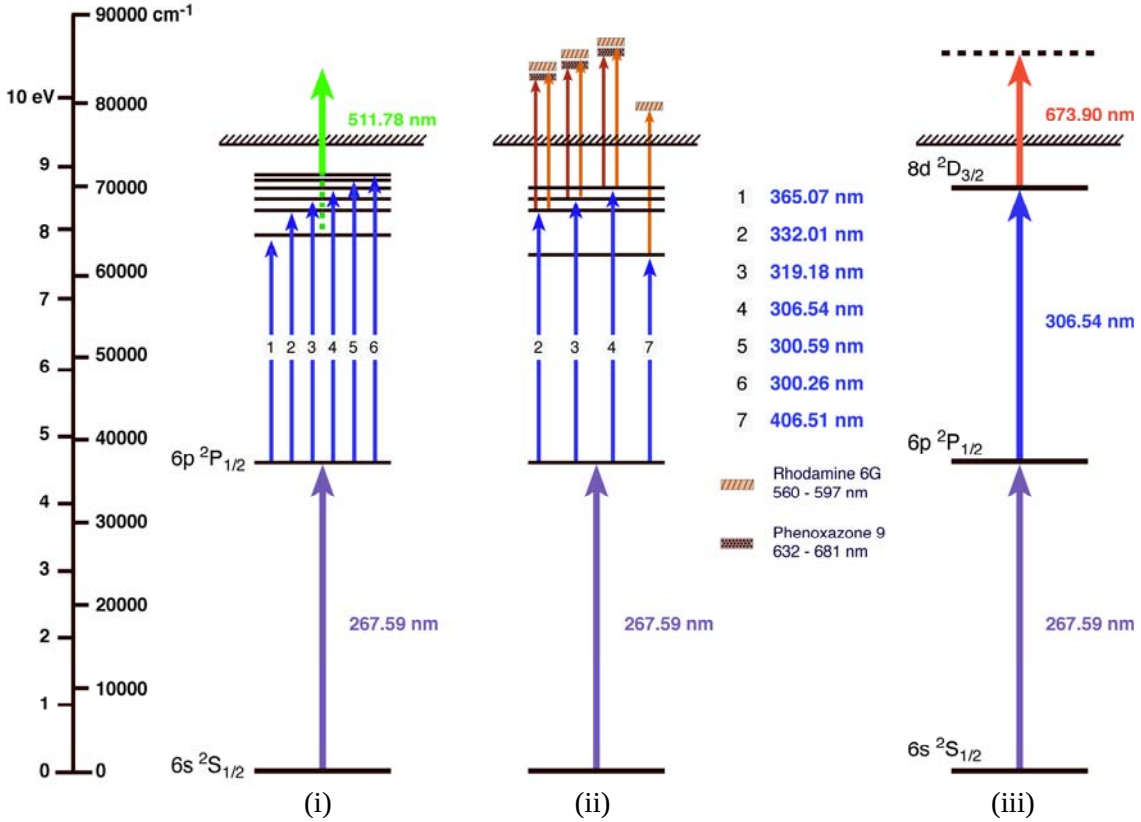

Figure 1. Ionization scheme development for Au:

(i) Investigating the relative strengths of the second step transitions.
(ii) Investigating third step transitions to an AIS for the schemes with strong second step transitions.

For the second phase of the study a search for auto-ionizing states was conducted. The CVL power used for the ionization stage was diverted to pump a third dye laser and dye amplifier. Ethanol solutions of the laser dyes Rhodamine 6G and Phenoxazone 9 were used in this laser, respectively the wavelength was scanned in the ranges of 560-597 nm and 632-681 nm. When an observable increase of the ion current was detected, scanning was stopped and the wavelength was optimized to the maximal value of the ion current. Its peak value, corresponding transition frequency, and values of laser power for each of three beams were recorded. Measurements of the laser frequency were produced with the wavelength meter of HighFinesse/Ånstrom model WS/7. The accuracy of the transition frequency measurements was defined by the width of resonance and laser line width (~ 0.6 cm^{-1}). For narrow AIS it was possible to define the peak position with the accuracy of about 0.1 cm^{-1}. Energy regions above the ionization threshold for the transitions from the second excited states corresponding to the four strongest second step transitions were studied.

A summary of these measurements is given in table 1. Within the energy intervals that were studied, 5 auto-ionizing states (AIS) had been previously observed [4, 7], but not as resonant transitions from the excited states measured during this study. Three of the known AIS were confirmed and 27 new AIS were observed. Figure 2 shows the profiles of the resonances for the two strongest AIS, at 84806.3 cm^{-1}(a) and 84880.4 cm^{-1}(b).

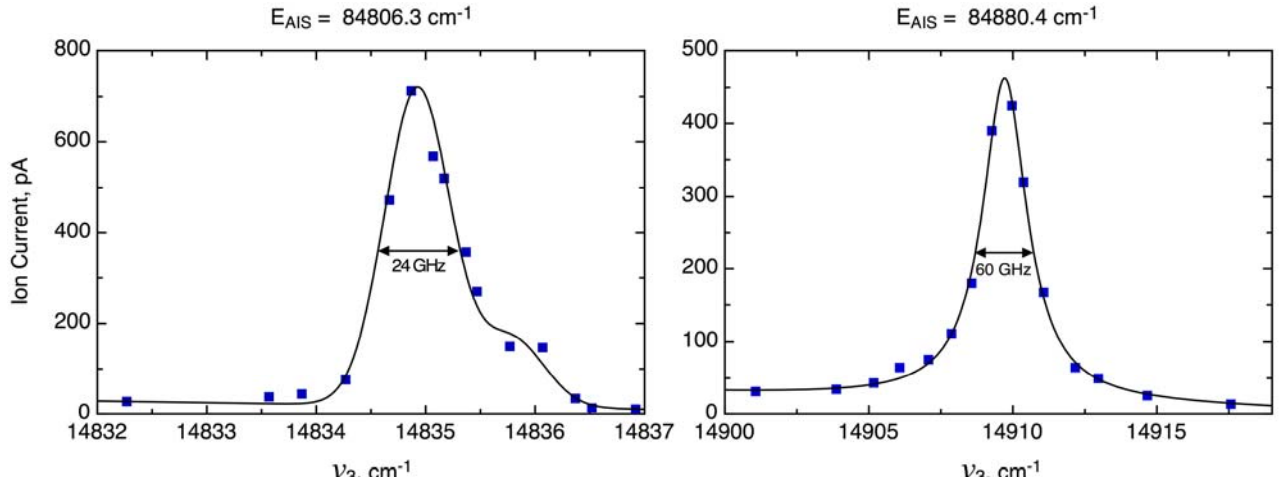

Figure 2. Resonance profiles for the two strongest AIS observed

Of particular interest was the measurement of a previously applied ionization scheme for Au [4]. This scheme, shown in italics in Table 1, was one of the more efficient schemes previously measured however the optimum scheme, shown on the right hand side of Figure 1, gives a factor of 4-5 increase in the efficiency parameter ***R***. The saturation measurements for the first and second step in this scheme are presented in Figure 3, they confirm that the saturation points for the transitions are exceeded with the laser power available.

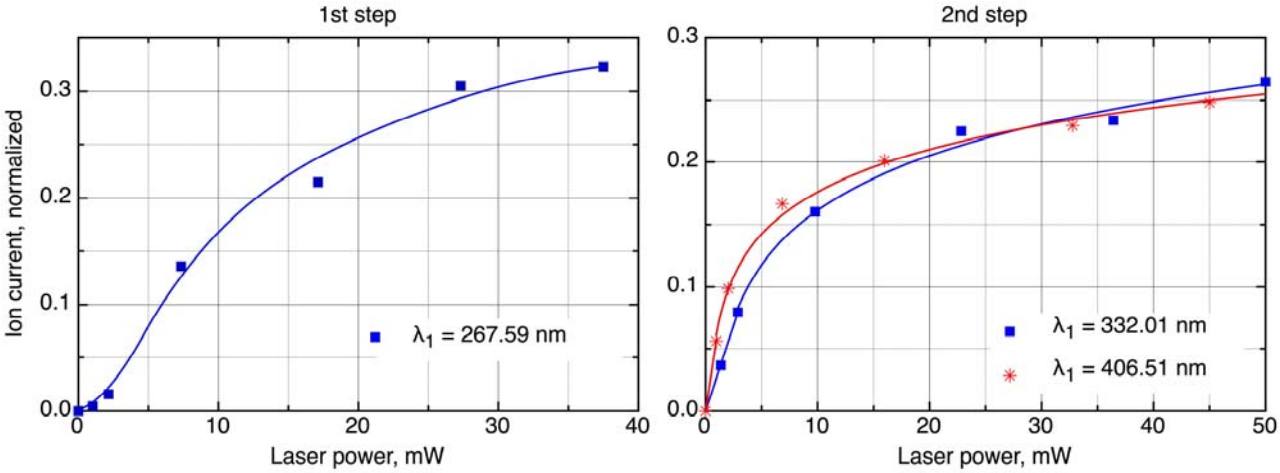

Figure 3. Saturation measurements of the first step and the two strongest second step transitions.

For the measurement of the absolute value of ionization efficiency, some experimental difficulties were encountered, limiting the reliability of the assessment of the mass marker evaporation. During the initial search for a resonance ionization signal, a large quantity of the Au sample was evaporated from the first oven. After detection of the ion signal, the subsequent tests were carried out without the need to heat the mass marker itself, evaporation of the gold that had condensed in the target container provided a sufficient and steady supply of gold vapor for the duration of the spectroscopic work. An attempt was made to extinguish this supply by gradually increasing the target heating from 2100 - 2400 K. A small decrease in

the ion current was observed after some hours. The evaporation of the 3000 nAh mass marker was then carried out with the target heating kept at approximately 2400 K. For improved laser ionization stability and experimental ease, only the first step laser was used for ionization during the efficiency measurement. The ionization efficiency of the scheme presented in Figure 1 was estimated to be over 3% by comparing the product of the ion current integration and the parameter ***R*** of the most efficient ionization scheme with the original sample size.

Table 1. The ionization schemes measured during this work. The values given for the laser power correspond to the power in the ion source measured by reflecting laser beams back to the laser setup.

λ_2 (air)	E_2	State II	λ_3 (air)	E_3	Laser Power, mW		***R***
nm	cm^{-1}		nm	cm^{-1}	Step 2	Step 3	
365.07	64742.90	8s $^2S_{1/2}$	511, 578	Continuum	75	10000	1.0
332.01	67469.68	7d $^2D_{3/2}$	511, 578	Continuum	75	10000	9.6
319.18	68680.63	9s $^2S_{1/2}$	511, 578	Continuum	60	10000	2.1
306.54	69971.42	8d $^2D_{3/2}$	511, 578	Continuum	75	11000	7.7
300.59	70617.73	10s $^2S_{1/2}$	511, 578	Continuum	65	11000	1.5
300.26	70653.25	5d^9 ($^2D_{5/2}$) 6s7s J=3/2	511, 578	Continuum	65	11000	1.2
406.51	*61951.89*	*6d $^2D_{3/2}$*	*591.90*	*78842.0*	*75*	*625*	*55*
319.18	68680.63	9s $^2S_{1/2}$	668.65	83631.9	90	1130	4.4
319.18	68680.63	9s $^2S_{1/2}$	644.93	84181.9	90	1130	3.1
332.01	67469.68	7d $^2D_{3/2}$	592.85	84332.8	90	500	10
332.01	67469.68	7d $^2D_{3/2}$	584.84	84563.8	90	750	6.4
332.01	67469.68	7d $^2D_{3/2}$	578.38	84754.5	90	550	73
306.54	69971.42	8d $^2D_{3/2}$	676.27	84754.3	80	750	150
332.01	67469.68	7d $^2D_{3/2}$	576.64	84806.6	90	950	120
306.54	**69971.42**	**8d $^2D_{3/2}$**	**673.90**	**84806.3**	**80**	**750**	**220**
332.01	67469.68	7d $^2D_{3/2}$	574.20	84880.5	90	750	34
306.54	69971.42	8d $^2D_{3/2}$	670.55	84880.4	80	1000	180
306.54	69971.42	8d $^2D_{3/2}$	666.24	84976.9	80	1130	13
332.01	67469.68	7d $^2D_{3/2}$	570.77	84985.0	90	750	2.6
306.54	69971.42	8d $^2D_{3/2}$	665.81	84986.6	80	1130	38
332.01	67469.68	7d $^2D_{3/2}$	569.80	85014.7	90	975	3.5
332.01	67469.68	7d $^2D_{3/2}$	567.24	85094.1	90	600	4.5
306.54	69971.42	8d $^2D_{3/2}$	661.08	85093.9	80	1250	21
332.01	67469.68	7d $^2D_{3/2}$	567.12	85097.8	90	600	5.4
306.54	69971.42	8d $^2D_{3/2}$	660.90	85098.0	80	1250	20
332.01	67469.68	7d $^2D_{3/2}$	564.14	85190.8	90	450	3.3
306.54	69971.42	8d $^2D_{3/2}$	632.80	85769.9	80	500	4.3
319.18	68680.63	9s $^2S_{1/2}$	567.39	86300.3	80	750	4.5
319.18	68680.63	9s $^2S_{1/2}$	565.61	86355.6	85	625	3.8
319.18	68680.63	9s $^2S_{1/2}$	565.36	86363.5	85	625	3.6
306.54	69971.42	8d $^2D_{3/2}$	575.60	87339.7	85	750	76
306.54	69971.42	8d $^2D_{3/2}$	572.38	87437.6	85	750	59
306.54	69971.42	8d $^2D_{3/2}$	570.70	87488.4	85	750	59
306.54	69971.42	8d $^2D_{3/2}$	567.98	87572.8	85	700	44
306.54	69971.42	8d $^2D_{3/2}$	567.14	87598.7	85	550	7.4
306.54	69971.42	8d $^2D_{3/2}$	564.07	87694.9	85	550	15
306.54	69971.42	8d $^2D_{3/2}$	561.71	87769.1	85	375	4.3

E_0 = 0 cm^{-1}; E_1 = 37358.99 cm^{-1}; State I = 6p $^2P_{1/2}$.

4 Conclusion

With the development of this new ionization scheme for gold, the RILIS can now provide a means of efficient and selective ionization of 26 of the elements. In accordance with the requirements of the ISOLDE experimental program, new schemes will continue to be developed for RILIS using procedures similar to those described in this work. Currently, such studies have to fit into the framework of general ISOLDE off-line development and thus, the dedicated mass separator use required is limited to just a few weeks per year. A recent letter of intent addressed to the INTC, "Development of the RILIS research laboratory at ISOLDE" gives details of a new and dedicated RILIS research laboratory. Following the completion of this laboratory, the investigation of new ionization schemes will become a task that is independent of ISOLDE scheduling. Many of the RILIS ionization schemes rely on an inefficient final step of non-resonant ionization using a large proportion of the total CVL power. It is hoped that the time consuming search for auto-ionizing states for many of these elements could be carried out in this laboratory and significant improvements in RILIS efficiency could be made.

5 Acknowledgements

The target preparation (assembly, mass marker preparation and initial testing) was carried out by R. Catherall, D. Carminati, B. Crepieux and T. Stora (CERN-AB). This work was supported by the EU 6th programme "Integrating Infrastructure Initiative – Transnational Access", Contract number: RII3-CT-2004-506065.

References

[1]. V.I. Mishin, V.N. Fedoseyev, H.-J. Kluge, V.S. Letokhov, H.L. Ravn, F. Scheerer, Y. Shirakabe, S. Sundell, O. Tengblad, the ISOLDE Collaboration, Nucl. Instrum. Methods Phys. Res. B **73**, 550 (1993).

[2]. V.N. Fedoseyev, G. Huber, U. Köster, J. Lettry, V.I. Mishin, H.L. Ravn, V. Sebastian, the ISOLDE Collaboration, Hyperfine Interactions **127**, 409 (2000).

[3]. E.B. Saloman, Spectrochimica Acta Part B **45**, 37 (1990).

[4]. U. Krönert, St. Beckert, Th. Hilberath, H.-J. Kluge, C. Schulz, Appl. Phys. A **44**, 339 (1987).

[5]. U. Krönert, St. Beckert, G. Bollen, M. Gerber, Th. Hilberath, H.-J. Kluge, G. Passler, ISOLDE Collaboration, Nucl. Instrum. Methods Phys. Res. A **300**, 522 (1991).

[6]. G.I. Bekov, A.T. Tursunov, G. Khasanov, N.B. Eshkobilov, Opt. Spectrosc. (USSR) **62**, 163 (1987).

[7]. W.Z. Zhao, X.Y. Xu, W.Y. Ma, Y. Cheng, Q. Hui, K.L. Wen, D.Y. Chen, Appl. Phys. B **52**, 299 (1991).

[8]. V.N. Fedosseev, D.V. Fedorov, R. Horn, G. Huber, U. Köster, J. Lassen, V.I. Mishin, M.D. Seliverstov, L. Weissman, K. Wendt, The ISOLDE Collaboration, Nucl. Instrum. Methods Phys. Res. B **204**, 353 (2003).

[9]. R. Catherall, V.N. Fedosseev, U. Köster, J. Lettry, G. Suberlucq, the ISOLDE Collaboration, B.A. Marsh, E. Tengborn, Rev. Sci. Instruments,

[10]. http://cfa-www.harvard.edu/amdata/ampdata/kurucz23/sekur.html

[11]. H.-P. Loock, L.M. Beaty, B. Simard, Phys. Rev. A **59**, 873 (1999).